Phase Diagram of Mixtures of Polymers in Aqueous Solution Using Fourier Transform Infrared Spectroscopy

C. Matin Durrani, David A. Prystupa, and Athene M. Donald*

Cavendish Laboratory, Department of Physics, University of Cambridge, Madingley Road, Cambridge CB3 0HE, U.K.

Allan H. Clark

Colworth House, Unilever Research, Sharnbrook, Bedford MK44 1LN, U.K.

Received July 9, 1992; Revised Manuscript Received November 12, 1992

ABSTRACT: A new method is presented to determine the phase diagram of mixed aqueous biopolymer systems using Fourier transform infrared spectroscopy coupled with partial least-squares analysis. We present the equilibrium phase diagrams of aqueous amylopectin/gelatin mixtures allowed to phase separate at a temperature outside the range within which either polymer could gel. The method is capable of detecting the changes in the phase diagram when the molecular weight of one of the components is altered. The phase diagrams are analyzed in terms of the Flory–Huggins theory for ternary systems. The method we have developed can be extended to any other combination of polymers in solution which show sufficient spectral difference.

Introduction

The behavior of mixtures of biopolymers in aqueous solution is important to the food industry in the search for new product types and for replacement materials for existing products.[1,2] Mixtures of polymers are generally immiscible,[3] and bulk phase separation into two distinct phases occurs in many mixed aqueous biopolymer systems of sufficient concentration.[4] Only over a limited range of concentrations do these biopolymer mixtures remain in a single bulk phase.[5] The purpose of a ternary phase diagram is to determine the conditions of miscibility and thereby establish how the solvent (water) partitions itself between the two phases.

Biopolymer mixtures are particularly useful to the food industry when either or both of the polymers can form a gel network. A biopolymer gel is a three-dimensional network of chains, held together through physical cross-links which extend across portions of the chains. A biopolymer gel also normally contains a large volume fraction of solvent. Aqueous gelatin gels, for example, have cross-links made from three helically entwined chains, stabilized through hydrogen bonding, and can be formed by cooling a gelatin solution with a concentration as low as ~1% (w/w) to room temperature.[6] In a biopolymer mixture which contains a gel-forming biopolymer, phase separation and gelation then become competing processes and the intervention of gelation introduces the possibility of nonequilibrium influences on the microscopic structure which is formed. One can therefore envisage the formation of a number of different structures, depending on the degree of miscibility of the polymers in solution, on the relative time scales of phase separation and gelation, and on the thermal regime which the mixture is subjected to. For example, mixed systems in which phase separation to equilibrium concentrations has been halted by gelation—as a result of cooling the system—have been observed.[7-9] In these systems a phase-separated structure is formed which consists of a continuous supporting phase containing inclusions of the other phase. If equilibrium has not been reached in the gel networks, one can expect time-related changes in the composition of each phase. Such systems are also observed to have a phase inversion at a particular concentration, at which the predominant component in the continuous and supporting phases changes over. In other mixed systems, bulk phase separation may take place first: any gelation can then occur subsequently and independently in each phase—provided the gelation occurs faster than the redistribution of polymers occurring due to the increasing molecular weight of species as the polymers aggregate. Gelation may also occur in the absence of any likely phase separation. Favorable interactions between chemically compatible regions of different chains can result in a coupled network, in which a single gel network is formed through a synergistic interaction between the two polymers.[10]

In tackling the question of water partitioning between phase-separated regions in a biopolymer mixture, Clark et al.[9] looked at phase-separated agar/gelatin mixtures which had gelled. They used the idea of complete demixing, controlled by a parameter measuring the relative affinity of the two phases for solvent, to calculate the local polymer concentration in each phase. These concentrations were then used to calculate the gel modulus of each phase on the basis of a cascade model for the relationship between the gel modulus and concentration. The isostress and isostrain approach to composite materials was used to work out the upper and lower bounds of the composite modulus. However, in this attempt to correlate mechanial behavior with microstructure, it was assumed that complete separation of the two polymer components into the separating phases was achieved. This assumption that each polymer is confined to a single phase is made merely to simplify the description, and there is no reason to suppose that such complete separation does indeed occur.

The variety of ways in which mixed biopolymer systems can act means that one can manipulate the mechanical behavior of the system. To be able to have such control requires not only an understanding of the gelation properties of the polymers but also a knowledge of the phase diagram. If gelation intervenes and proceeds too rapidly, it may not be possible to determine a true equilibrium phase diagram below the gelling temperature. However, if the phase diagram is determined at a temperature above the gelling temperatures of either polymer, the problem of gelation is removed and equilibrium conditions can be reached.

There are a number of existing techniques which have been used to plot phase diagrams of biopolymer mixtures

0024-9297/93/2226-0981$04.00/0

in water. They have relied on a variety of chemical, geometrical, or simple physical methods to plot out on a ternary diagram the concentrations in the two phases of samples left to separate to equilibrium. Performing a chemical analysis of the phases of a bulk phase separated mixture is perhaps the most obvious way of determining the concentrations in each phase—but a chemical analysis can only be used for those mixtures whose polymers have some existing test. Such analyses also require the removal of solvent from each phase prior to study. Kalichevsky and Ring[11] plotted the phase diagram of aqueous mixtures of amylose and dextran in which they determined the amylose content of each phase by freeze-drying both phases, dispersing them in dimethyl sulfoxide, and then using a standard chemical assay to determine the amylose "blue value". This drastic processing of the phases is time-consuming and likely to introduce large errors into the calculated concentrations.

A more refined yet still indirect technique to plot the phase diagram was used by Polyakov, Grinsberg, and Tolstogusov,[12] which they called the phase volume ratio method. It consisted of measuring the volumes of the two bulk phase separated phases in a calibrated capillary tube, before using a graphical calculation involving a geometrical analysis to determine the weight fraction of the two polymers in each phase.

The increase in the amount of light scattered by a mixed system at the cloud point during the transition from the one- to the two-phase region as polymer is added has been used to plot phase diagrams.[13] Sometimes it is combined with optical rotation methods.[14] Determining the concentrations at which the cloud points occur however leads to a map of the coexistence curve, which may not be the map of the concentrations in the phases of mixtures left to separate to equilibrium. This method has the added disadvantage that it does not give the tie lines and cannot therefore predict how a given mixture will separate.

The method we describe here uses Fourier transform infrared (FTIR) spectroscopy to plot the phase diagram. We believe it to be the first reported use of this technique to plot the phase diagram of an aqueous biopolymer mixture. It proves to be a fast, accurate, reliable, and nondestructive way of directly probing the composition of the phases.

A report in the literature uses infrared spectroscopy to map out the phase diagram of a synthetic polymer blend.[15] The method of Bhagwagar et al. was based on measuring the relative sizes of the "free" and the hydrogen-bonded carbonyl absorption bands within the amide I region of an aromatic polyamide blended with a polyether. Because a change with temperature in the size of the hydrogen-bonded carbonyl band compared to the free carbonyl band was observed, and because polyamide self-association increases the number of hydrogen-bonded carbonyl groups, this suggested that the blend had separated upon heating into polyamide-rich and polyamide-deficient regions. These researchers used a calculation of the relative amounts of the two types of carbonyls to plot a temperature–composition phase diagram. The calculation not only required measurement of the areas of the two absorption bands but also relied upon the experimental determination of the absorptivity ratio of the two peaks. Furthermore, to be sure they were dealing with phase-separated blends, these researchers needed to calculate the interassociation equilibrium constant and show it to be different from the theoretical value for a single phase blend. This method has the severe limitation that it relies on the existence of specific interactions together with a theory to describe the changes in these interactions as the composition changes. It is therefore a specific rather than a general method, and also does not deal with the case of a ternary system. By contrast, the method we have developed should have wide applicability and does not require some specific quirk. It simply relies on there being some spectral difference between each polymer constituent.

The development of FTIR spectrometers, which produce data in a digital form, has facilitated quantitative measurements and fostered the development of a host of numerical analytical methods. Among these is the partial least-squares (PLS) method of analysis which is used in the present study. The PLS method is based on taking the spectra of a series of standards of known concentration to form a matrix of calibration spectra—whose elements are the infrared absorbance at each experimentally sampled frequency for each spectrum—and then using this matrix to predict the concentrations in samples of unknown concentration.

Previous infrared studies of aqueous biopolymer systems have been limited by the fact that many of the key absorption bands of the biopolymers are obscured by the strong absorption of water. This problem has customarily been skirted by replacing H_2O with D_2O, and this is the approach taken in the present study. Although there is the possibility that using D_2O rather than H_2O as the solvent influences the results by introducing a slight isotopic effect, we do however know for instance that the melting temperature of a gelatin gel is increased by only 1.5 °C when the solvent is changed from H_2O to D_2O.[16]

The biopolymer mixture studied here is the amylopectin/gelatin/D_2O system. Both amylopectin and gelatin form gels when a sufficiently concentrated solution is cooled. Gelatin is a protein derived from animal connective tissue. Its properties have been widely studied over the years with a large number of different techniques,[6] and it is well-known that in solution it behaves as a random coil, with gelation involving the formation of triple helical junction zones when such a solution is cooled to temperatures below ~35 °C. Amylopectin is a polysaccharide which is found in starch and is responsible for the crystallinity inherent in starch granules.[17] It is a highly and nonrandomly branched polymer whose precise internal structure is complex and difficult to determine.[18,19] However, amylopectin is a commercially relevant biopolymer which has great practical significance: this mixed system is therefore a highly pertinent one for investigation.

In this paper the phase diagram of the amylopectin/gelatin/D_2O system at 51 °C is presented, i.e., above the gel temperature of either constituent. The effect of changing the molecular weight of the amylopectin on the phase diagram is investigated. The time evolution of the concentrations of polymers in the phases has also been followed to ensure that equilibrium has been reached. It will be seen that the assumptions about complete phase separation of the two polymer constituents which are commonly made[9,20] are incorrect.

Experimental Section

Sample Preparation. Commercial food-grade gelatin and amylopectin samples were obtained from Unilever, and D_2O (99.9% isotopic purity) was bought from Aldrich Chemical Co., Dorset. Two fractions of amylopectin of different molecular weight were used to plot two separate gelatin/amylopectin/D_2O phase diagrams. The amylopectin fractions were prepared by pyrolysis of waxy maize starch under dry acid conditions for different periods of time. Both fractions dissolved easily in water

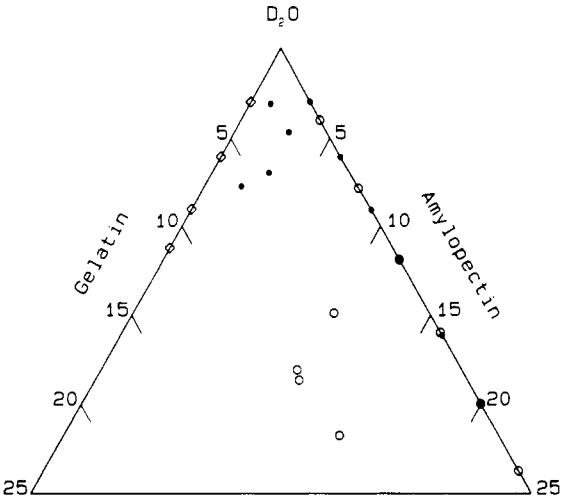

Figure 1. Concentrations of the standards whose spectra were used in the calibration matrices of the partial least-squares analysis shown on a ternary diagram: (○) standards containing the lower molecular weight amylopectin; (●) standards containing the higher molecular weight amylopectin; (◊) standards consisting purely of gelatin in D_2O. The standards were made up on the basis of weight percentages and are expressed as such on the diagram.

at temperatures above ~70 °C. The biopolymers were used without further treatment.

Samples were made by weighing out the appropriate masses of amylopectin, gelatin, and D_2O into a sealed bottle. All samples were calculated on a weight percentage basis. Samples were left overnight at room temperature to allow the gelatin to swell, and were then heated to 85 °C for 10 min while being mixed with a magnetic stirring bar.

The calibration matrix used in the PLS method must contain the infrared spectra not only of standards which are single component systems but also of mixed systems—since the chemical interactions of one component with another are liable to alter the infrared spectrum of a mixture. Furthermore, the standards must also cover the concentration range which one expects to analyze. The concentrations of the calibration standards which were therefore used to form the calibration matrix for each phase diagram are given in Figure 1. The same pure gelatin solution standards were able to be used for both diagrams since the PLS method predicts each component individually. However, amylopectin solutions and amylopectin/gelatin mixtures were made separately for both amylopectin molecular weights.

Whereas mixed solutions intended for calibration were used immediately in order to preempt any possible phase separation, mixed solutions which were intended for plotting the phase diagram were transferred to small glass vials and left to phase separate in an oven at 51 °C. Solvent loss was prevented by coating the ground-glass joints of the vials with silicon vacuum grease.

Samples of the top and bottom phases formed during phase separation in the oven were extracted in succession from mixtures left for 24 h and injected into Specac semipermanent liquid cells which were made up of two 4-mm CaF_2 windows separated by a 12.5-μm tin spacer. Cells were preheated to 51 °C before injecting the samples. Infrared spectra were recorded with a Mattson 4020 FTIR spectrometer equipped with a DGTS detector. The spectrometer was well purged with dry nitrogen gas. For each sample, 100 interferograms recorded at 4-cm^{-1} resolution were coadded and Fourier transformed using Beer–Norton strong apodization.

Data Reduction and PLS Analysis. Polymer concentrations in phase-separated samples were estimated by the partial least-squares (PLS) method using Advanced First software supplied by Mattson. A detailed and well-documented description of this method is given by Haaland and Thomas.[21]

The PLS method is a pattern recognition technique which can be applied to the quantitative analysis of experimental data. It uses the patterns measured from calibration mixtures whose components are of known concentration to predict concentrations in mixtures of unknown composition. In our case the patterns are the spectral data sets of infrared absorbance at each experimentally sampled frequency. The PLS algorithm reduces the matrix of calibration spectra into the product of two smaller matrices. The first matrix is made up of basis vectors for a new coordinate system, each of which is optimized for concentration prediction. The number of such basis vectors used to represent each component in the new coordinate system is specified by the user (see below) to capture the best predictive ability without overfitting the data. The other matrix is one of spectral absorbances whose values are related to concentration. It is used to calculate concentration in the mixtures of unknown composition.

Although the PLS algorithm is a full-spectrum method, considerable computational effort is spared by limiting the analysis to the region(s) which contains information from the chemical components of interest. For the present study a single range, 980–2000 cm^{-1}, was selected. This range included amide bands from the gelatin in the 1500–1700-cm^{-1} range and peaks from amylopectin between 1000 and 1100 cm^{-1}. These were in addition to a D_2O peak centered on 1212 cm^{-1} and smaller bands from HDO and H_2O arising from hydrogen exchange between D_2O and the two biopolymers. Specific designations of particular bands are not required by the method. However, assignments for the spectra of both biopolymers are given in the literature.[22,23]

The initial idea was to use the PLS method to predict the concentrations of gelatin, amylopectin, and D_2O individually. This approach suffered from two weaknesses. Firstly, the viscosity of the samples was such that the samples could not be removed from the cell without disassembling it. This inevitably resulted in a variation in path length from one sample to the next. One of the implicit assumptions of the PLS model is that any changes in absorption between spectra are only due to changes in concentration and not to differences in path length. Secondly, a three-component model does not account for the correlation between concentration specified by the conservation of mass. If two of the concentrations are predicted, the third can be trivially determined. Furthermore, modeling three components rather than two requires more parameters and would be liable to increase the uncertainty in the predictions.

Both of these drawbacks were overcome by the following method. To compensate for changes in sample thickness, the spectral data of both the standards and the unknowns were normalized by setting the lowest absorption in the range 980–2000 cm^{-1} to zero and then scaling the D_2O peak at 1120 cm^{-1} to an absorption of unity. The PLS algorithm was then used to predict the ratios of gelatin to D_2O and amylopectin to D_2O. We note that in this way the D_2O, together with the CaF_2 windows, and any HDO and H_2O were modeled implicitly as the background. The concentration of D_2O was calculated from the conservation of mass.

An estimate of the optimal number of basis vectors was obtained from a prediction error sum of squares (PRESS) calculation carried out by the PLS method. Generally, to get a model which predicts concentrations most accurately, the number of basis vectors which gives a minimum in PRESS is selected. In the phase diagram containing the lower molecular weight amylopectin, the number of basis vectors was 3 for the gelatin/D_2O component and 4 for the amylopectin/D_2O component. In the phase diagram containing the higher molecular weight amylopectin, it was 3 for the gelatin/D_2O and 6 for the amylopectin/D_2O component.

To confirm that these choices of basis vectors were the best, we looked closely at the results of the cross-calibration method, which is one of the options in the PLS method. The cross-calibration method is one which performs the PLS calibration using the selected basis vectors on all the calibration spectra bar one, and uses this calibration to predict the concentration of the one sample left out of the calibration. The process is repeated until each sample has been left out once and its concentration predicted. We found that the sum of the absolute differences between the predicted and acutal concentrations of the calibration samples was at a minimum when the basis vectors which gave a minimum in PRESS were chosen. The results from the cross-calibration also allowed "outliers" to be spotted—that is, any standard whose predicted concentration clearly was not close to

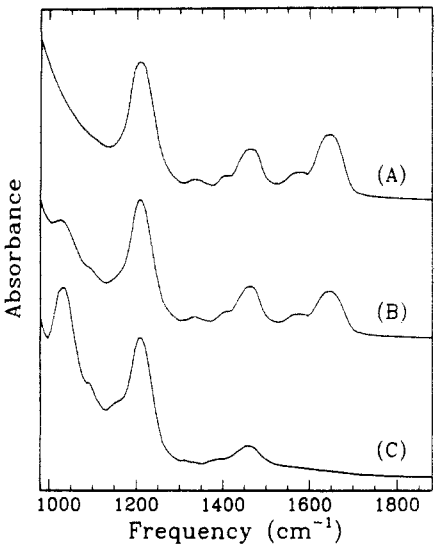

Figure 2. Fourier transform infrared spectra of three of the standards: (A) gelatin in D_2O (11.2% (w/w)); (B) mixture of gelatin (8.4%) and amylopectin (10.2%) in D_2O (81.4%); (C) amylopectin in D_2O (20.0% (w/w)). All three spectra are shown in the form in which they were used in the calibration matrices, with the lowest point in the region between 980 and 2000 cm^{-1} having been set to zero and the data having been scaled so that the D_2O peak at 1212 cm^{-1} was set to an absorbance of unity.

the actual concentration. In our case the presence of any outliers was noted, and these standards were remade and repeated.

Results

The FTIR spectra of amylopectin in D_2O, gelatin in D_2O, and a mixture of amylopectin and gelatin in D_2O are shown in Figure 2. The spectra are shown in the form in which they were used by the PLS method—with the lowest point in the spectrum in the region 980–2000 cm^{-1} having been set to zero and the spectrum having been scaled so that the absorbance of the D_2O peak at 1120 cm^{-1} is unity.

Although the separation of mixtures into two visually distinct phases occurred within 2 h, it was initially uncertain whether equilibrium had necessarily been reached by that time. To establish the time required for the concentrations in the two phases to reach their equilibrium values, a mixture was subdivided into different vials and the spectrum of each phase at different times was taken. Using the PLS method to predict concentrations, it was deduced that leaving samples before study for a minimum of 24 h was sufficient time to ensure that equilibrium conditions had been reached. Figure 3 shows the constancy of the predicted concentration in the top phase of a mixture beyond 24 h. We can therefore be confident that our results represent equilibrium conditions.

The phase diagrams of mixed aqueous biopolymer systems containing amylopectin and gelatin in D_2O at 51 °C are given in Figures 4 and 5. Figure 4 was made with the higher molecular weight amylopectin sample and Figure 5 with the lower molecular weight amylopectin. In both mixed systems phase separation into a gelatin-rich upper phase and an amylopectin-rich lower phase took place. The points on the curves represent the weight concentrations in the top and bottom phases as determined by our PLS method. Both phase diagrams also include the composition of the starting samples. The tie line drawn through each set of three compositions (representing the starting composition, the top phase, and the bottom phase) is calculated by a least-squares best fit to the three data points.

The error in the data points can be evaluated using the results from the cross-validation method. This gives the

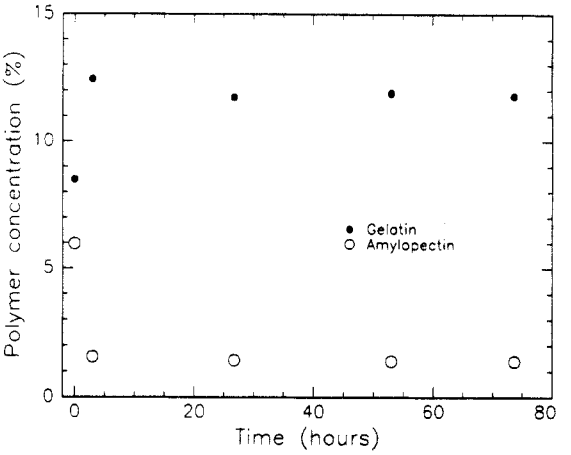

Figure 3. Time dependence of the concentrations of gelatin and amylopectin in the top phase of a mixed system which has phase separated. The concentrations are those predicted by our method. The constancy in the concentrations beyond 24 h shows that leaving samples for 24 h was sufficient time to ensure that equilibrium conditions had been reached.

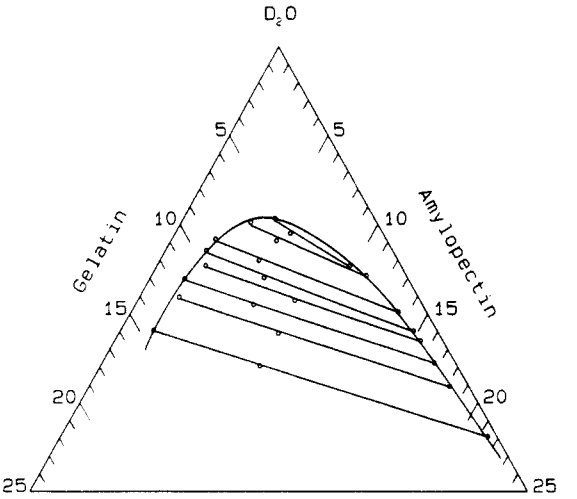

Figure 4. Ternary phase diagram of the mixed system containing gelatin, the higher molecular weight fraction of amylopectin, and D_2O. Concentrations are weight percentages. The tie line through each set of three points is the least-squares best fit to the data. The point in the middle of each line represents the concentration of the starting mixture. The point at the left end of each line is the concentration in the top phase of the mixture when left to phase separate for 24 h. The point at the right end of each line is the concentration in the bottom phase of the mixture when left to phase separate for 24 h.

errors in the predicted concentrations of the calibration standards compared to their actual concentrations, on the basis—as explained above—of performing a calibration on all the standards bar one and using this calibration to predict the concentration of the standard which has been left out. Given that the aim of the PLS method is to predict the concentrations in unknown samples, the cross-calibration results give us the most reliable estimate of the prediction errors. Using these results, the absolute errors in the concentrations of the standards, in terms of the ratio of polymer to D_2O, had a standard deviation of 1.3×10^{-3} for the PLS matrix containing the higher molecular weight amylopectin and 6.4×10^{-3} for the one containing the lower molecular weight amylopectin. Individually, however, the gelatin/D_2O component was better predicted than the amylopectin/D_2O component in both diagrams, with the standard deviation being only 1.4×10^{-3} for the gelatin/D_2O component, 1.5×10^{-3} for the higher molecular weight amylopectin/D_2O component, and 8×10^{-3} for the lower molecular weight amylopectin/D_2O component. The

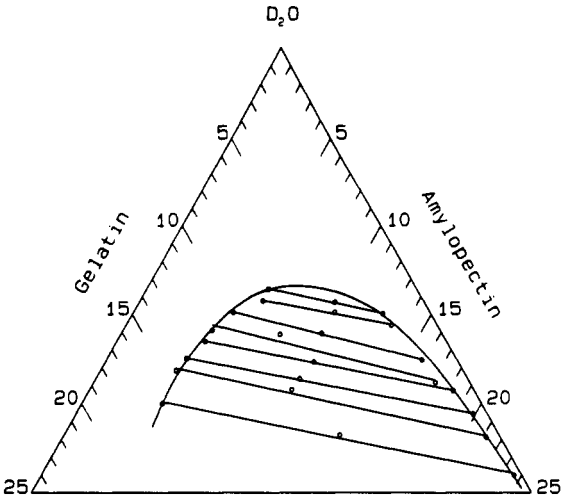

Figure 5. Ternary phase diagram of the mixed system containing gelatin, the lower molecular weight fraction of amylopectin, and D_2O. Concentrations are weight percentages. The line through each set of three points is the least-squares best fit to the data. The effect of a decrease in molecular weight of the amylopectin (cf. Figure 4) is to shift the apex of the phase boundary toward the amylopectin corner of the phase diagram and increase the area of the one-phase region.

relative errors will however be smaller at higher concentrations, indicating that the predictive power of the method is best at higher polymer concentrations.

We could also have taken advantage of the fact that the calibration matrix for the phase diagram containing one of the amylopectin molecular weight samples could have been used for the phase diagram containing the other amylopectin, since the infrared absorption is dependent on the number of monomers present, i.e., concentration. However, we thought it preferable to create a set for each.

Discussion

The method we have developed involving the use of PLS software is seen to work very well. The shape of the curve separating the one- and two-phase regions is essentially similar to that of phase diagrams determined by existing techniques for other systems. A clear indication that the method is very successful is the fact that the best fit straight line through each set of three points passes closely through each set: a straight tie line connecting the points is expected by the lever rule. The starting compositions for phase diagrams of this type, determined using the other techniques outlined earlier, are often not included or are not even accessible.[4,11,13,14]

Both phase diagrams are assymetric and are skewed toward the branched amylopectin component. The effect of a decrease in molecular weight of the amylopectin is to shift the apex of the curve toward the amylopectin corner of the phase diagram and to increase the area of the one-phase region on the phase diagram. The gelatin-rich top phase is capable of containing more of the lower molecular weight amylopectin than it can of the higher molecular weight amylopectin. This is to be expected on thermodynamic grounds. The lower amylopectin-rich phase appears to be similar in both phase diagrams in that it is capable of supporting less of the other polymer than the top phase can. However, it is clear that complete demixing has not occurred in either phase.

On the phase diagram containing the lower molecular weight amylopectin (Figure 4), the tie lines are approximately parallel to one another with a root-mean-square deviation about the mean slope of the lines of only 1.19°. However, on the phase diagram containing the higher molecular weight amylopectin, the slopes of the tie lines increase as the concentrations of the end points of the tie lines move up the phase boundary, such that the lines appear to "rotate". This effect has been observed in other protein/polysaccharide systems.[5]

The quality of these results permits an analysis of them by the Flory–Huggins model of polymer solutions. Tie line calculations based on the Flory–Huggins model for a two-polymer/one-solvent system were performed using the iterative minimization procedure described previously by Hsu and Prausnitz.[24] In this approach polymer molecular weight polydispersity and the effect of the branching of the amylopectin were ignored. The independent parameters of the treatment were the effective volume ratios of gelatin and amylopectin with respect to water (V_G and V_A) and the Flory–Huggins interaction parameters for gelatin with respect to solvent (χ_{GS}), amylopectin with respect to solvent (χ_{AS}), and gelatin with respect to amylopectin (χ_{GA}). The χ values were treated as constants at a fixed temperature, i.e., independent of polymer concentration. In the fitting of tie line data, the phase diagram information of Figures 4 and 5 was converted from mass fraction to volume fraction terms using values of 0.707 and 0.620 mL/gm for the partial specific volumes of gelatin[25] and amylopectin, respectively.[26]

The volume ratios of the polymer in relation to the solvent were in the first instance treated as equivalent to the number-average degree of polymerization (DP_n) values (but see later comment). The DP_n value appropriate to our particular gelatin sample is at present unknown, and is therefore a variable of the fit, but estimates of DP_n for the two amylopectin samples are available from experimental NMR end group analysis. These were 400 ± 100 for the higher molecular weight amylopectin and 150 ± 50 for the lower molecular weight amylopectin. These values were introduced as constants into the fitting procedure to overcome correlation problems involving the molecular volume variables and the interaction parameter χ_{GA}. Therefore, V_G, χ_{GS}, χ_{AS}, and χ_{GA} were varied systematically in the fitting procedure, and a best fit was achieved for each tie line individually.

For the phase diagram for the lower molecular weight amylopectin, final estimates designed to give an overall fit to all eight tie lines were obtained by averaging the values obtained for each individual tie line, together with some further manual adjustment to optimize the fit. (Overall fitting of the tie lines by a systematic least-squares procedure was not possible, at the present time, because of computational difficulties involving periodic failure in convergence of the Hsu and Prausnitz procedures.) Final values for the parameters, and the nature of the fit to the phase diagram containing the lower molecular weight amylopectin, appear in Figure 6.

To describe the diagram appropriate to the mixed system containing the higher molecular weight amylopectin fraction, a first attempt at the calculating procedure involved simply using the values for the three χ parameters and for V_G which were obtained in the fit for the phase diagram for the lower molecular weight amylopectin, and the DP_n estimate of 400 for this amylopectin fraction. This, in effect, provided a zero parameter prediction of the behavior of the higher molecular weight amylopectin with gelatin in aqueous solution. The result is shown in Figure 7. Clearly the prediction is only approximately correct, as it tends to overestimate the increase in insolubility which occurs as the molecular weight of the amylopectin increases.

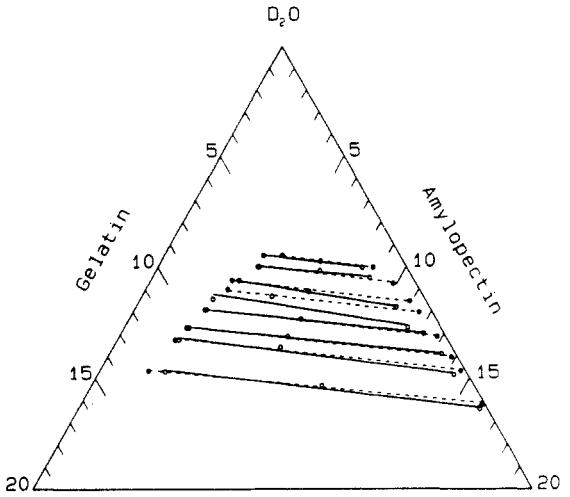

Figure 6. Phase diagram data of Figure 5 containing the lower molecular weight amylopectin shown converted from weight percentages to volume percentages (using values for the partial specific volumes of amylopectin and gelatin given in the text). Also shown are the results of tie line calculations, based on the Flory-Huggins model for a two-polymer/one-solvent system, given the starting concentration of each mixture. The starting concentrations and the concentrations in the two phases as predicted by our method are shown as open circles, and the continuous line is the least-squares best fit throught each set of three points. The concentrations in the phases from the Flory–Huggins tie line calculation are shown by filled circles, and the dashed line is the least-squares best fit line through these points and the corresponding starting concentrations. In this fit, $V_A = 150$ and $V_S = 1$ were fixed; χ_{GS}, χ_{AS}, χ_{GA}, and V_G were variables of the fit. Final values for the parameters in this fit were $V_G = 560$, $\chi_{GS} = 0.46$, $\chi_{AS} = 0.51$, and $\chi_{GA} = 0.082$.

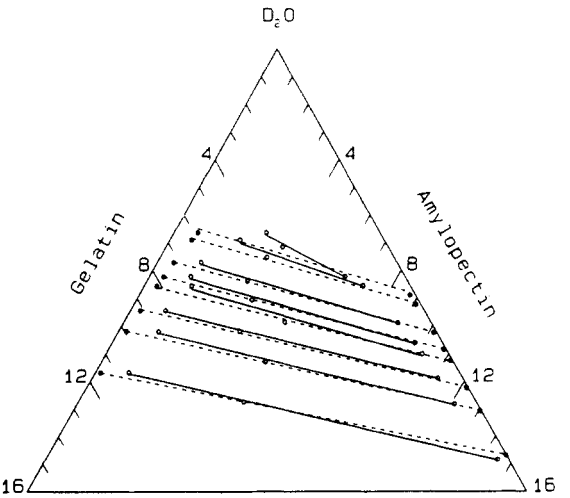

Figure 7. Phase diagram data of Figure 4 containing the higher molecular weight amylopectin shown converted from weight percentages to volume percentages (using values for the partial specific volumes of amylopectin and gelatin given in the text). Also shown are the results of tie line calculations, based on the Flory–Huggins model for a two-polymer/one-solvent system, given the starting concentration of each mixture. The meaning of the symbols and lines is the same as in Figure 6. In this calculation, the same parameters which were used successfully for the phase diagram containing the lower molecular weight amylopectin were used, except that the new experimental estimate for V_A was set to 400. The prediction is only approximately correct.

Refinement of the model was possible in two ways. One, which was physically somewhat unreasonable, was to allow both polymer volume ratios to vary until a good fit to the data was achieved (Figure 8). The fit however required a contradiction between the estimates for the gelatin DP_n from one system to another. This was unsatisfactory. The

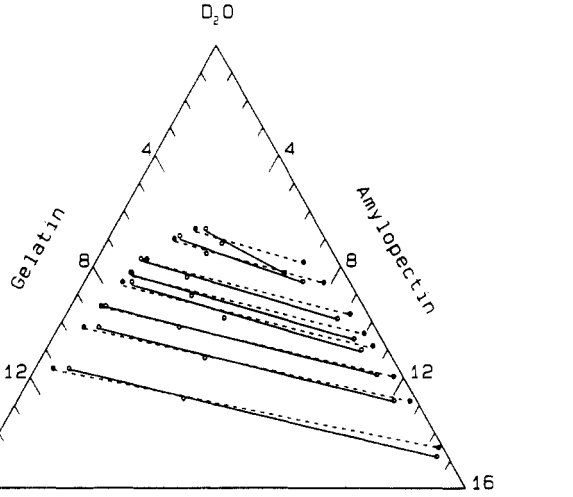

Figure 8. Data of Figure 4 containing the higher molecular weight amylopectin, converted to volume percentages as in Figure 7. Also shown are the results of tie line calculations, based on the Flory–Huggins model for a two-polymer/one-solvent system, given the starting concentration of each mixture. In the fit here, the polymer volume ratios, V_A and V_G, were made variables of the fit. The other parameters were all set at the values used in the fits of Figures 6 and 7: $V_S = 1$, $\chi_{GS} = 0.46$, $\chi_{AS} = 0.51$, and $\chi_{GA} = 0.082$. The final values for V_A and V_G were 300 and 400, respectively. This is unsatisfactory because it would have meant that the molecular weight of the gelatin was different in the two phase diagrams.

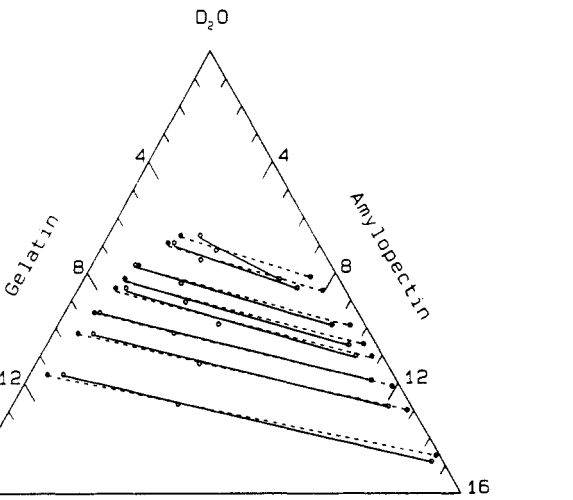

Figure 9. Data of Figure 4 containing the higher molecular weight amylopectin, converted to volume percentages as in Figure 7. Also shown are the results of tie line calculations, based on the Flory–Huggins model for a two-polymer/one-solvent system, given the starting concentration of each mixture. The meaning of the symbols and lines is the same as in Figure 6. In this fit, the condition that the χ values are independent of molecular weight has been relaxed. The same parameters as in Figure 7 were used: $V_S = 1$, $V_G = 560$, $V_A = 400$, $\chi_{GS} = 0.46$, and $\chi_{AS} = 0.51$ were all fixed. To produce the fit, only χ_{GA} needed adjustment. A final value of $\chi_{GA} = 0.059$ was obtained.

other approach was to relax the condition that the χ values should be independent of molecular weight and to allow them to be variables of the fit. In fact only χ_{GA} needed adjustment, to give the fit shown in Figure 9. This second option is physically reasonable because the amylopectin molecules vary in degree of branching, and the ideal theory does not in fact consider branched molecules at all. An important result to emerge from carrying out this analysis is that the polymer/solvent χ values for gelatin and amylopectin (0.46 and 0.51) are not far from recent literature estimates (0.48 and 0.50) based on second virial coefficients.[25,27,28] From the nature of the fitting procedure

it is difficult to give accurate ranges of uncertainty for the χ values obtained here, but they are certainly as large as the differences just noted. Finally, it is interesting that fits which are comparable to those presented in Figures 6–9 can be obtained by converting the DP's to more correct molecular volume ratios with respect to water—i.e., taking into account the considerable differences in volume between polymer segments and water molecules. Similar results for χ_{GS} and χ_{AS} emerge, but of course higher values for V_G and V_A (compared again to experimental estimates) and lower values for χ_{GA} are produced. Once again it is necessary to change χ_{GA} as one moves from lower to higher molecular weight amylopectin. It is also interesting that while the whole analysis can be performed on a percentage weight for weight basis for the phase diagrams, this procedure leads to a value of $\chi_{GS} \approx 0.4$ which is unrealistically low.

Conclusions

Phase diagrams for mixed aqueous biopolymer systems using a method based on Fourier transform infrared spectroscopy coupled with partial least-squares analysis are reported for the first time. We present the equilibrium phase diagram of an aqueous amylopectin/gelatin mixture allowed to phase separate at a temperature (51 °C) outside the range at which either polymer could gel, and show that the method is capable of detecting the changes in the phase diagram when the molecular weight of one of the components is altered. The effect of a decreased molecular weight amylopectin is, as expected, to shift the phase boundary down and to increase the area of the one-phase region. The method we have developed has the additional advantage that either phase diagram can now be repeated at different temperatures, without the need for any recalibration, to investigate the effect of this variable on the phase diagram. The method could also be used to look at the effect of ionic strength and pH on the phase diagram provided a new set of calibration standards are prepared. We know all these variables can strongly affect the degree and range of miscibility in mixed biopolymer systems.[5]

The results have been analyzed in terms of the Flory–Huggins model applied to a ternary polymer system. A good fit to the data for the phase diagram containing the lower molecular weight amylopectin, gelatin, and D_2O was achieved, given an experimental estimate for the molecular weight of the amylopectin and allowing the χ values and the gelatin molecular weight to vary. The fit produced χ values for amylopectin and gelatin in water which agree well with literature values. In order to fit the data of the phase diagram containing the higher molecular weight amylopectin, apart from the need to use the different experimental amylopectin molecular weight estimate, only the χ interaction parameter was altered. That this should be different in the two cases is not surprising, given that amylopectin varies in its degree of branching with molecular weight and that the Flory–Huggins theory does not treat branched polymers at all.

We have in addition demonstrated the practicality of the partial least-squares method of analysis in the field of aqueous biopolymer mixtures. We believe that our method can now be routinely applied to investigate the phase behavior of a wide range of other mixed polymer systems, including mixtures in other solvents. The only proviso is that the polymers show sufficient spectral difference. It can also be used to investigate the effect of temperature, pH, and ionic strength on the phase diagram. The method could also be adapted to study binary polymer blends. This method has also shown that the question of water partitioning in mixed aqueous systems can be investigated. Our next aim is to use FTIR microscopy to look at phase separation on a local scale in samples cooled to room temperature which gel before bulk phase separation is allowed to take place. By looking at the concentration fluctuations, we can study the partitioning of water between microphase-separated structures.

Acknowledgment. The authors are grateful to the Agriculture and Food Research Council for funding this work and for providing a Ph.D. studentship to C.M.D. in cooperation with Unilever. We are also grateful to Dr. M. J. Gidley of Unilever Research for providing us with DP_n estimates for the amylopectin samples.

References and Notes

(1) Brownsey, G. J.; Morris, V. J. In *Food Structure-Its Creation and Evaluation*; Blanshard, J. M. V., Mitchell, J. R., Eds.; Butterworth: London, 1988.
(2) Aguilera, J.; Kessler, H. *J. Food Sci.* **1989**, *54*, 1213–1218.
(3) Manson, J. A.; Speling, L. H. *Polymer Blends and Composites*; Heyden Press: London, 1976.
(4) Antonov, Y. A.; Pletenko, M. G.; Tolstoguzov, V. B. *Polym. Sci. USSR (Engl. Transl.)* **1987**, *29*, 2724–2729.
(5) Tolstoguzov, V. B. In *Functional Properties of Food Macromolecules*; Mitchell, J. R., Ledward, D. A., Eds.; Elsevier: London, 1986; pp 385–415.
(6) Djabourov, M. *Contemp. Phys.* **1988**, *29*, 273–297.
(7) Kalichevsky, M. T.; Orford, P. D.; Ring, S. G. *Carbohydr. Polym.* **1986**, *6*, 145–154.
(8) Watase, M.; Nishinari, K. *Biorheology* **1983**, *20*, 495–505.
(9) Clark, A. H.; Richardson, R. K.; Ross-Murphy, S. B.; Stubbs, J. M. *Macromolecules* **1983**, *16*, 1367–1374.
(10) Cairns, P.; Miles, M. J.; Morris, M. J. *Carbohydr. Res.* **1987**, *160*, 411–423.
(11) Kalichevsky, M. T.; Ring, S. G. *Carbohydr. Res.* **1987**, *162*, 323–328.
(12) Polyakov, V. I.; Grinberg, V. Y.; Tolstoguzov, V. B. *Polym. Bull.* **1980**, *2*, 757–760.
(13) Perrau, M. B.; Iliopolous, I.; Audebert, R. *Polymer* **1989**, *30*, 2112–2117.
(14) Piculell, L.; Svante, N.; Falck, L.; Tjerneld, F. *Polymer* **1991**, *32*, 158–160.
(15) Bhagwagar, D. E.; Panter, P. C.; Coleman, M. M.; Krizan, T. D. *J. Polym. Sci., Part B: Polym. Phys.* **1991**, *29*, 1547–1558.
(16) Prystupa, D. A. Personal Communication.
(17) Blanshard, J. M. V. In *Starch: Properties and Potential*; Galliard, T., Ed.; John Wiley and Sons: Chichester, U.K., 1987; Vol. 13.
(18) Robin, J. P.; Mercier, C.; Charbonniere, R.; Guilbot, A. *Cereal Chem.* **1974**, *51*, 389–405.
(19) Burchard, W.; Thurn, A. *Macromolecules* **1985**, *18*, 2072–2082.
(20) Morris, E. R. *Carbohydr. Polym.* **1992**, *17*, 65–70.
(21) Haaland, D. M.; Thomas, E. V. *Anal. Chem.* **1988**, *60*, 1193–1202.
(22) Milch, R. A. *Nature* **1964**, *202*, 84–5.
(23) Goodfellow, B. J.; Wilson, R. H. *Biopolymers* **1990**, *30*, 1183–1189.
(24) Hsu, C. C.; Prausnitz, J. M. *Macromolecules* **1974**, *7*, 320–334.
(25) Pezron, I.; Herning, T.; Djabourov, M.; Leblond, J. In *Physical Networks: Polymers and Gels*; Burchard, W., Ross-Murphy, S. B., Eds.; Elsevier Applied Science: London and New York, 1990; pp 231–252.
(26) Lips, A.; Hart, P. M.; Evans, I. D.; Debet, M. In *Gums and Stabilisers for the Food Industry*; Phillips, G. O., Williams, P. A., Wedluck, D. J. Eds.; Oxford University Press: New York, 1992; Vol. 6, pp 335–342.
(27) Ring, S. G.; I'Anson, K. J.; Morris, V. J. *Macromolecules* **1985**, *18*, 182–188.
(28) Roger, P.; Colunna, P. *Carbohydr. Res.* **1992**, *227*, 73–83.